# MONTE CARLO RAY-TRACING APPROACH TO EFFECTIVELY DESIGN THE ELLIPSOIDAL REFLECTOR OF SOLAR SIMULATORS


**Marco Bortolini[a], Mauro Gamberi[b], Alessandro Graziani[c], Riccardo Accorsi[d], Emilio Ferrari[e]**

[a],[c],[d],[e]Department DIEM – Industrial Mechanical Plants, University of Bologna,
Viale Risorgimento 2, 40138 Bologna, Italy
[b]Department of Management and Engineering, University of Padova,
Stradella San Nicola 3, 36100 Vicenza, Italy

[a]marco.bortolini3@unibo.it, [b]mauro.gamberi@unipd.it, [c]alessandro.graziani6@unibo.it,
[d]riccardo.accorsi2@unibo.it, [e]emilio.ferrari@unibo.it



## ABSTRACT

Solar simulators are widely adopted devices to artificially reproduce the emission spectrum of the Sun. Their use, in lab tests and analyses, allows to study the effect of solar radiation on both materials and components. This paper focuses on the effective design of the ellipsoidal reflector for concentrating solar simulators. A Monte Carlo ray-tracing approach is proposed to study the reflector geometric configuration maximizing the target incident radiation and optimizing the radiative incident flux distribution. Developed ray-tracing model includes the main physical and optic phenomena affecting light rays from the source to the target area, e.g. absorption, deviation, reflection, distortion, etc. Proposed model is integrated to a Monte Carlo simulation to properly design the ellipsoidal mirror reflector of a small scale solar simulator based on an OSRAM XBO® 3000W/HTC OFR Xenon short arc lamp as light emitting source. Several scenarios are tested and the main obtained evidences are summarized.



Keywords: solar simulator, ray-tracing, Monte Carlo simulation, reflector surface design


## 1. INTRODUCTION

Solar simulators provide a luminous flux approximating natural sunlight spectrum. Their basic structure includes a metal support frame, a light source, e.g. high flux arc lamp with power supplier and igniter, and a reflective surface to properly orient the emitted rays lighting the target area. The reflector shape allows the system to generate a concentrated or non-concentrated light beam through an ellipsoidal or parabolic reflector. Figure 1 shows an example of concentrating solar simulator structure, highlighting the main functional modules.

The relevance of such systems, in lab tests and analyses, is frequently discussed by the recent literature presenting several applications for a wide set of research fields. Petrash et al. (2007) both review the topic and describe a 11,000 suns high-flux solar simulator. Domínguez et al. (2008), Domínguez et al. (2009), Pravettoni et. al. (2010), Rehn and Hartwig (2010), Hussain et al. (2011) and Meng et al. (2011a)

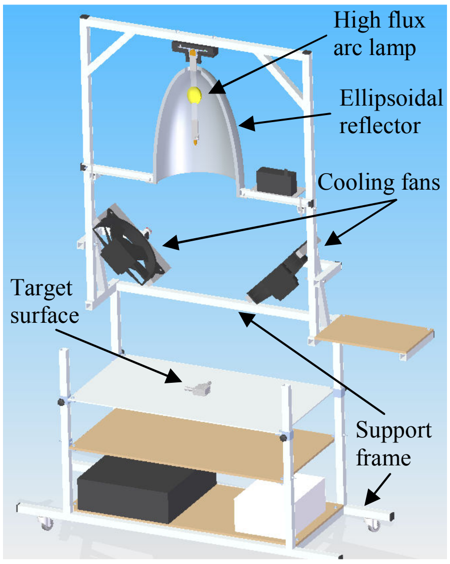


Figure 1: Single Lamp Solar Simulator, Main Functional Modules

present different studies about the design and development of high flux solar simulators applied to both concentrating and non-concentrating photovoltaic systems. Amoh (2004) and Meng et al. (2011b) describe the design of solar simulators to test multi-junction solar cells for terrestrial and space applications. Kreuger et al. (2011) develop a 45 kW solar simulator for high-temperature solar thermal and thermo-chemical researches, while Codd et al. (2010) present a low cost high flux simulator to study the optical melting and light absorption behavior of molten salts. All these contributions focus on the relevance of the proper design of the system to achieve high performances in both flux intensity and uniformity on the target area. Mirror reflective surface represents a crucial component to gain these purposes. An accurate shape design and simulation of the physical and optic properties is essential to the simulator construction (Johnston 1995).

Ray-tracing algorithms combined to Monte Carlo analyses are recognized as effective approaches to test the performances of different configurations of the reflective surface (Petrash et al. 2007, Chen et al. 2010, Ota and Nishioka 2010, Cooper and Steifeld 2011).

This paper presents an effective Monte Carlo ray-tracing approach to properly design the ellipsoidal reflector of concentrating solar simulators. Developed approach is applied to study the optimal shape of the ellipsoidal reflector for a small scale solar simulator based on a OSRAM XBO® 3000W/HTC OFR Xenon short arc lamp (http://www.osram.com). A description of the implemented approach is provided giving full details about the steps of the ray-tracing algorithm together with the simulated scenarios. Finally, the main obtained evidences are discussed.

The reminder of this paper is organized as follows: Section 2 describes the steps of the implemented ray-tracing model, Section 3 presents the Monte Carlo analysis to design the ellipsoidal reflector of solar simulators and introduces the developed case study. In Section 4, the case study results are discussed while Section 5 concludes this paper with suggestions for further research.

## 2. REFLECTOR OPTICAL DESIGN THROUGH RAY-TRACING APPROACH

In geometrical optics, the foci of an ellipsoid of revolution are conjugate points (Petrash et al. 2007). If no distortion effects occur, each ray emitted by a punctiform source located in one of the foci passes through the other after a single specular reflection (Figure 2).

According to this principle, concentrating solar simulators are designed. The light source, reproducing Sun emission spectrum, and the target area, e.g. the studied material or component, are located at the foci of an ellipsoidal mirror reflective surface.

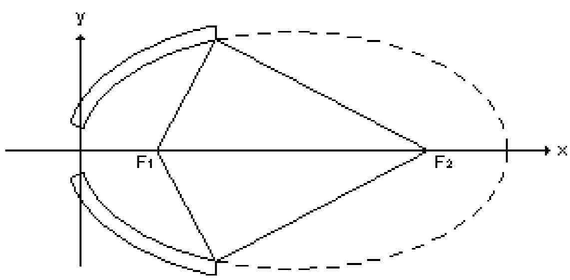


Figure 2: Geometrical Optic of Ellipsoid of Revolution

Considering experimental contexts, the following main conditions and phenomena contribute to reduce the global system radiation transfer efficiency, expressed as the ratio between the light flux that reaches the target and the global emitted flux.

- Finite area of the emitting light source.
- Absorption phenomena due to the presence of light source quartz bulb, source electrodes and reflective surface.
- Deviation and distortion phenomena due to the specular dispersion errors of the reflective surface.
- Losses due to rays falling out of the reflector shape.

These conditions affect all the operative contexts and can not be neglected in the solar simulator design. Their impact in reducing the system performances is strongly correlated to the features of the emitting source, the target shape and, particularly, to the reflector shape and characteristics.

Proposed ray-tracing approach analytically studies the ray trajectories, predicting the global transfer performances, given a configuration of the source, reflector and target surface. Figure 3 summarizes the step sequence of the proposed approach highlighting the stages where losses in transfer efficiency occur.

According to the major literature (Petrash et al. 2007, Domínguez et al. 2008, Kreuger et al. 2011) the light source is assumed to emit isotropic radiation uniformly from its surface. Consequently, the emission point, $P_0$, is randomly located on the whole source surface. Incident ray direction, **v**, is defined following Lambert's cosine law distribution, as expressed in Eq. (1) (Steinfeld 1991)

$$\mathbf{v} \times \mathbf{n} = \cos\left(\sin^{-1}\sqrt{U}\right) = \sqrt{1-U} \qquad (1)$$

where **n** is the normal direction to the emitting surface, in $P_0$, and $U$ a random number drawn from a [0,1] uniform distribution. Proper quartz bulb and electrodes absorption phenomena are considered by introducing two coefficients, i.e. bulb and electrodes absorption coefficients, that reduce the emitted radiation and decrease the system transfer efficiency, i.e. losses at the light source stage.

For each emitted ray, the point of intersection with the ellipsoidal surface, $P_1$, is computed. If $P_1$ falls out of the surface shape or in the hole necessary to install the light source, the ray is lost and the process finishes. Otherwise, two possibilities occur. Generally, the mirror reflects the ray but, in few cases, an absorption phenomenon occurs and the ray is not reflected at all. In this circumstance, modeled considering a proper absorption coefficient, the process ends, i.e. losses at the reflector stage.

Considering the reflected rays, their direction, **r**, needs to be estimated. Distortion effects, caused by the specular dispersion errors of the reflective surface, affect **r** vector. As widely discussed by Cooper and Steinfled (2011), geometric surface errors modify the normal vector, **k**, to the ellipsoid surface. The authors identify two angular components of the dispersion error, i.e. the azimuthal angular component, $\theta_{err}$, and the circumferential component, $\varphi_{err}$. By applying the, so called, Rayleigh method they outline proper expressions to estimate these angular errors.

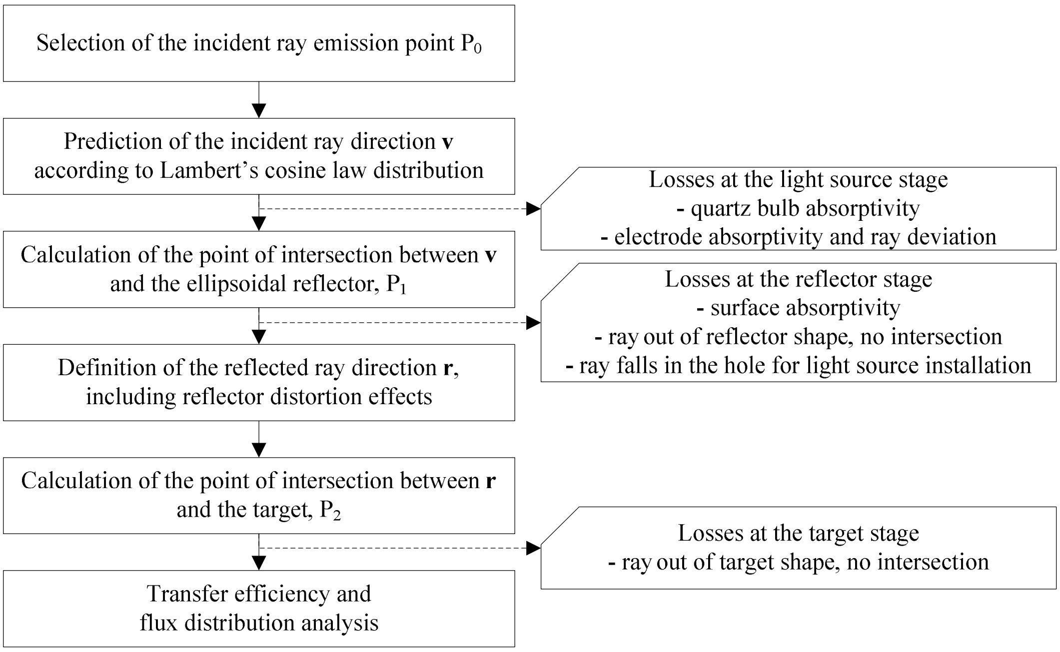

Figure 3: Steps and Losses of the Proposed Ray-Tracing Approach

$$\theta_{err} = \sqrt{2} \cdot \sigma_{err} \cdot \sqrt{-\ln U} \quad (2)$$

$$\varphi_{err} = 2\pi U \quad (3)$$

where $\sigma_{err}$ is the standard deviation of the dispersion azimuthal angular error distribution, including all distortion effects, and $U$ a random number drawn from a [0,1] uniform distribution.

As a consequence, to estimate the direction of **k**, in the point of intersection $P_1$, the theoretic normal vector **k'** needs to be twofold rotated with rotation angles equal to $\theta_{err}$ and, then, $\varphi_{err}$. $\theta_{err}$ rotation is around a vector orthogonal to the plane where the major ellipse lies while the second rotation is around **k'**.

The normal direction to the reflective surface, in $P_1$, allows to calculate the reflected ray direction, **r**, according to Eq. (4) (Steinfeld 1991).

$$\mathbf{r} = \mathbf{v} - 2 \cdot (\mathbf{k} \times \mathbf{v}) \times \mathbf{k} \quad (4)$$

The intersection between **r** and the plane where the target lies allows to calculate the coordinates of the common point $P_2$. If $P_2$ is inside the target area the ray correctly hits the target, otherwise the ray is lost and the transfer efficiency decreases, i.e. losses at the target stage. This study does not consider multiple reflection phenomena.

Finally, the distance and mutual position between $P_2$ and the ellipsoid focus point allows to study the radiative incident flux distribution on the target area.

## 3. MONTE CARLO SIMULATION

Several geometric and optic parameters affect the global transfer efficiency of solar simulator systems. A list of them, classified according to the physical component they belong to, is provided in follows.

Parameters of the light source (generally an high flux arc lamp):

- Shape and dimensions.
- Emission light spectrum.
- Emission surface shape and dimensions, e.g. sphere, cylinder, etc.
- Emission direction distribution.
- Absorption coefficients of quartz bulb and electrodes (if present).
- Interference angle of electrodes (if present).

Parameters of the ellipsoidal reflector:

- Reflector shape, identified by the two ellipsoid semi-axes or by the major semi-axis and the truncation diameter.
- Reflector length, i.e. the distance between the vertex, on the major axis, and the longitudinal truncation section.
- Absorption coefficient.
- Standard deviation of the dispersion azimuthal angular error distribution, previously called $\sigma_{err}$.

Parameters of the target surface:

- Shape, e.g. circular, squared, rectangular.
- Dimensions.
- Relative position toward the ellipsoid.

For a given a set of such parameters, the geometric and optical features of the solar simulator are univocally identified and the ray-tracing approach, described in previous Section 2, can be applied, cyclically, to study the system performances, simulating a large number of emitted light rays. Furthermore, varying one or several of these parameters, through a *what-if analysis*, the best configuration of the whole system can be pointed out.

The authors developed a customized *MatLab®* interface to speed the simulation process, calculate and represent the system transmission performances.

### 3.1. Case study. Design of a small scale solar simulator

The following case study provides an empirical application of the described ray-tracing approach and Monte Carlo design simulation strategy.

A small scale solar simulator is investigated. The overall structure of the plant is represented in previous Figure 1 and the main functional modules are shortly introduced in Section 1. In this context, the effective design of the ellipsoidal reflector is analyzed. Both the emitting source and target area features are assumed constant, while several configurations of the reflector shape, corresponding to different sets of parameters, are tested and performances compared.

The considered emitting source is an OSRAM XBO® 3000W/HTC OFR Xenon short arc lamp (http://www.osram.com) with a luminous flux of 130000 lumen and an average luminance of 85000 cd/cm$^2$. Other relevant data about the shape of the considered high flux lamp are summarized in Table 1 and shown in Figure 4.

Table 1: Key Features of the Emitting Source Shape. Refer to Figure 4 for Notations

| Light Source Parameters | | |
|---|---|---|
| Lamp length (overall) | $l_1$ | 398mm |
| Lamp length | $l_2$ | 350mm |
| Lamp cathode length | a | 165mm |
| Electrode gap (cold) | eo | 6mm |
| Bulb diameter | d | 60mm |
| Electrode interference angles | $\vartheta_1$ | 30° |
| | $\vartheta_2$ | 20° |

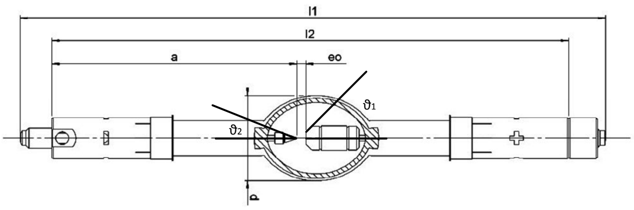


Figure 4: High Flux Emitting Source, Structure and Notations

The target surface is squared, side length of 50 mm, and it lies on a plane located on one of the two foci of the ellipsoidal reflector, orthogonal to the ellipsoid major axis.

Considering the ellipsoidal mirror reflector, the next Table 2 and related Figure 5 summarize all the tested scenarios, providing the adopted ranges of variation and the considered incremental steps for the four following parameters defining the reflector shape and optic features:

- Ellipsoid major semi-axis length, $A$
- Ellipsoid truncation section diameter, $TD$
- Standard deviation of the dispersion azimuthal angular error distribution, $\sigma_{err}$
- Reflector length, i.e. the distance between the vertex, on the major axis, and the longitudinal truncation section, $L$

Table 2: Tested Configurations for the Ellipsoidal Reflector. Refer to Figure 5 for Notations

| Reflector Parameters [mm] | | | |
|---|---|---|---|
| | Min | Max | Step |
| $A$ | 200 | 1000 | 100 |
| $TD$ | 100 | $2A$ | 50 |
| $\sigma_{err}$ | 0.005 | 0.01 | 0.005 |
| $L$ | $A-\sqrt{A^2-TD^2/4}$ | $A$ | 50 |

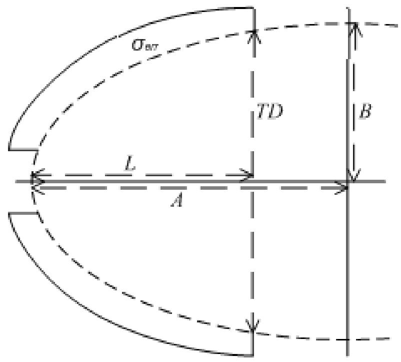


Figure 5: Ellipsoidal Reflector, Shape and Notations

The minor semi-axis of the ellipsoid, called $B$ in Figure 5, can be analytically calculated as

$$B = \frac{A \cdot TD}{2\sqrt{L(2A-L)}} \tag{5}$$

and it is not a free parameter to define the ellipsoid shape.

Furthermore, a constant mirror absorption coefficient of 4% is considered in the analysis.

3840 scenarios appear and need to be simulated, i.e. *what-if analysis*. For each scenario, $N = 5{\times}10^5$ emitted rays are traced and results collected.

## 4. CASE STUDY RESULTS AND DISCUSSION

The following data are collected in all tested scenarios.

- $N_A$, number of rays absorbed by the light source (quartz bulb and electrodes).
- $N_H$, number of rays lost due to the presence of the hole used to install the light source.
- $N_L$, number of rays falling out of the reflector shape.
- $N_R$, number of rays absorbed by the mirror reflector.
- $N_T$, number of reflected rays hitting the target.
- $N_O$, number of reflected rays that do not hit the target.

These data allow to measure the role played by the ellipsoidal reflector shape on the global optic performances.

Furthermore, the following key indices are calculated to highlight the impact of the reflector features on the solar simulator transfer efficiency.

- Losses due to the reflector shape, i.e. ellipsoid shape, hole and truncation diameters.

$$\xi_1 = \frac{N_H + N_L}{N - N_A} \tag{6}$$

- Losses due to the optic and distortion effects caused by the reflector surface errors.

$$\xi_2 = \frac{N_R + N_O}{N - N_A - N_H - N_L} \tag{7}$$

- Global reflector transfer efficiency.

$$\eta = (1 - \xi_1) \cdot (1 - \xi_2) = \frac{N_T}{N - N_A} \tag{8}$$

- Statistical distribution of the reflected rays on the target surface, i.e. the mean distance $M_D$ and standard deviation $\sigma_D$ of the point of intersection between the rays and the target, $P_2$, and the ellipsoid focus point.

Table 3 shows an example of the obtained results presenting the twenty best and worst scenarios. In addition to previous notations, $\varepsilon$ indicates the ellipsoidal reflector eccentricity, defined as

$$\varepsilon = \sqrt{1 - B^2/A^2} \tag{9}$$

and included in the $[0,1]$ range.

Figure 6 shows a radiative flux map for the best scenario. The squared dashed line identifies the target area whereas all dots inside the square are the rays that correctly hit the target, while the other dots are the rays causing the losses at the target stage (see Figure 3).

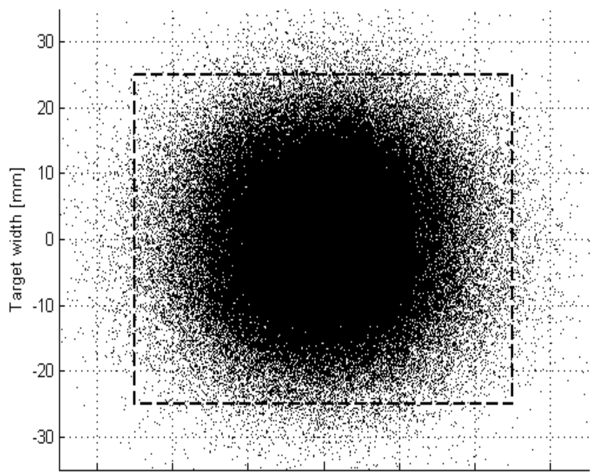


Figure 6: Radiative Flux Map for the Best Scenario.

Values of the global transfer efficiency vary from 92.407% of the best scenario to 1.072% of the worst case. Consequently, a first relevant outcome of the analysis is the heavily influence, for solar simulator performances, of the reflector design. Considering the best scenarios of Table 3, the $\xi_1$ and $\xi_2$ loss indices have values lower than 9% while the large amount of the rays are concentrated close to the target, i.e. mean distance between rays and the ellipsoid focus point, $M_D$, close to 10 mm and standard deviation, $\sigma_D$, included between $[5,13]$ mm. On the contrary, the main cause for the performance decrease are the losses due to the reflector shape. With reference to the worst scenarios of Table 3, high values of $\xi_1$, greater than 93%, are always experienced while $\xi_2$ does not present a regular trend. The main reason for these losses is the critic length of the reflector, i.e. the parameter $L$. All worst scenarios have very small values for this parameter, e.g. 50 or 100 mm, so that a great number of the emitted rays are lost because they do not hit the mirror reflector. The very high value of the number of rays falling out of the reflector shape, $N_L$, included between the 80% and 86%, clearly highlights the main cause for the global transfer efficiency decrease.

The standard deviation of the dispersion azimuthal angular error distribution, previously identified as $\sigma_{err}$, represents another relevant parameter affecting the global performances of the system. As expected, low values of $\sigma_{err}$ correspond to high global transfer efficiency values. However, to reduce the standard deviation error an increase of the reflector production costs is necessary because of the major accuracy required during reflector manufacturing and mirror surface treatments. The graph in Figure 7 correlates the reflector length to the global transfer efficiency for the two simulated values of $\sigma_{err}$, i.e. 0.005 mm and 0.01 mm. The obtained values are listed in Table 4.

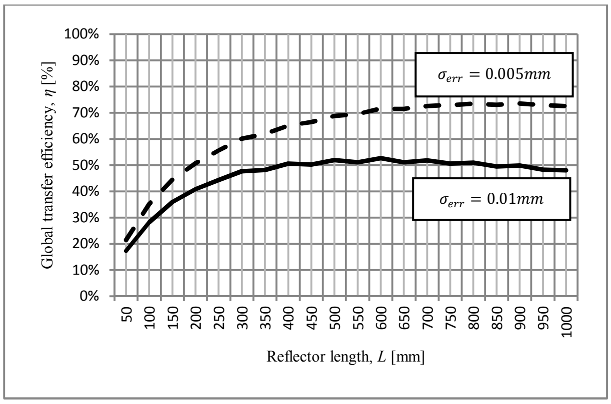


Figure 7: Correlation between the Reflector Length and Global Transfer Efficiency for the Two Values of $\boldsymbol{\sigma_{err}}$.

Results, for the tested two values of the standard deviation of the dispersion azimuthal angular error distribution, present similarities in the waveforms. Low values of the reflector length are associated to very poor

Table 3: *What-if Analysis* Results. Twenty Best and Worst Scenarios.

| *Rank* | *A* | *TD* | $\sigma_{err}$ | *L* | *B* | $\varepsilon$ | $N_A$ | % | $N_H$ | % | $N_L$ | % | $N_R$ | % | $N_T$ | % | $N_o$ | % | $\xi_1$ | $\xi_2$ | $\eta$ | $M_D$ | $\sigma_D$ |
|---|---|---|---|---|---|---|---|---|---|---|---|---|---|---|---|---|---|---|---|---|---|---|---|
| 1 | 600 | 650 | 0.005 | 600 | 325 | 0.841 | 65506 | 13.10% | 5585 | 1.12% | 6771 | 1.35% | 16942 | 3.39% | 401501 | 80.30% | 3695 | 0.74% | 2.844% | 4.889% | 92.407% | 8.284 | 6.387 |
| 2 | 700 | 700 | 0.005 | 700 | 350 | 0.866 | 65865 | 13.17% | 6287 | 1.26% | 719 | 0.14% | 16935 | 3.39% | 399723 | 79.94% | 10471 | 2.09% | 1.614% | 6.416% | 92.073% | 9.867 | 7.265 |
| 3 | 700 | 750 | 0.005 | 700 | 375 | 0.844 | 65477 | 13.10% | 2107 | 0.42% | 5849 | 1.17% | 17211 | 3.44% | 399732 | 79.95% | 9624 | 1.92% | 1.831% | 6.291% | 91.993% | 9.622 | 7.147 |
| 4 | 600 | 600 | 0.005 | 600 | 300 | 0.866 | 65943 | 13.19% | 13355 | 2.67% | 702 | 0.14% | 16782 | 3.36% | 399052 | 79.81% | 4166 | 0.83% | 3.239% | 4.988% | 91.935% | 8.521 | 6.205 |
| 5 | 600 | 700 | 0.005 | 600 | 350 | 0.812 | 65936 | 13.19% | 1491 | 0.30% | 13675 | 2.74% | 16838 | 3.37% | 398989 | 79.80% | 3071 | 0.61% | 3.494% | 4.753% | 91.919% | 8.077 | 7.453 |
| 6 | 500 | 550 | 0.005 | 500 | 275 | 0.835 | 65626 | 13.13% | 12034 | 2.41% | 7907 | 1.58% | 16699 | 3.34% | 396935 | 79.39% | 799 | 0.16% | 4.591% | 4.222% | 91.381% | 6.918 | 5.108 |
| 7 | 500 | 600 | 0.005 | 500 | 300 | 0.800 | 65623 | 13.12% | 4064 | 0.81% | 16235 | 3.25% | 16688 | 3.34% | 396752 | 79.35% | 638 | 0.13% | 4.673% | 4.184% | 91.338% | 6.705 | 5.281 |
| 8 | 700 | 800 | 0.005 | 700 | 400 | 0.821 | 65424 | 13.08% | 499 | 0.10% | 11629 | 2.33% | 17004 | 3.40% | 396659 | 79.33% | 8785 | 1.76% | 2.791% | 6.105% | 91.275% | 9.462 | 7.226 |
| 9 | 600 | 650 | 0.005 | 550 | 326 | 0.839 | 65174 | 13.03% | 5308 | 1.06% | 13451 | 2.69% | 16698 | 3.34% | 395752 | 79.15% | 3617 | 0.72% | 4.314% | 4.883% | 91.014% | 8.298 | 6.631 |
| 10 | 700 | 700 | 0.005 | 650 | 351 | 0.865 | 65824 | 13.16% | 6088 | 1.22% | 5619 | 1.12% | 16789 | 3.36% | 395000 | 79.00% | 10680 | 2.14% | 2.696% | 6.502% | 90.977% | 9.868 | 7.868 |
| 11 | 700 | 750 | 0.005 | 650 | 376 | 0.844 | 65819 | 13.16% | 1925 | 0.39% | 11180 | 2.24% | 16775 | 3.36% | 394742 | 78.95% | 9559 | 1.91% | 3.018% | 6.254% | 90.916% | 9.661 | 12.983 |
| 12 | 600 | 600 | 0.005 | 550 | 301 | 0.865 | 65393 | 13.08% | 13003 | 2.60% | 6290 | 1.26% | 16493 | 3.30% | 394753 | 78.95% | 4068 | 0.81% | 4.439% | 4.951% | 90.830% | 8.508 | 6.197 |
| 13 | 800 | 800 | 0.005 | 800 | 400 | 0.866 | 65306 | 13.06% | 2336 | 0.47% | 744 | 0.15% | 17232 | 3.45% | 394171 | 78.83% | 20211 | 4.04% | 0.709% | 8.675% | 90.678% | 11.228 | 8.321 |
| 14 | 600 | 750 | 0.005 | 600 | 375 | 0.781 | 65675 | 13.14% | 286 | 0.06% | 21051 | 4.21% | 16654 | 3.33% | 393652 | 78.73% | 2682 | 0.54% | 4.913% | 4.682% | 90.635% | 7.923 | 10.472 |
| 15 | 800 | 850 | 0.005 | 800 | 425 | 0.847 | 65715 | 13.14% | 659 | 0.13% | 5146 | 1.03% | 17002 | 3.40% | 392510 | 78.50% | 18968 | 3.79% | 1.337% | 8.395% | 90.381% | 11.004 | 8.655 |
| 16 | 600 | 700 | 0.005 | 550 | 351 | 0.811 | 65720 | 13.14% | 1407 | 0.28% | 21106 | 4.22% | 16375 | 3.28% | 392244 | 78.45% | 3148 | 0.63% | 5.184% | 4.741% | 90.321% | 8.074 | 6.300 |
| 17 | 700 | 850 | 0.005 | 700 | 425 | 0.795 | 65720 | 13.14% | 211 | 0.04% | 17598 | 3.52% | 16642 | 3.33% | 392119 | 78.42% | 7710 | 1.54% | 4.101% | 5.847% | 90.292% | 9.232 | 10.141 |
| 18 | 700 | 650 | 0.005 | 650 | 326 | 0.885 | 65836 | 13.17% | 13360 | 2.67% | 584 | 0.12% | 16704 | 3.34% | 391884 | 78.38% | 11632 | 2.33% | 3.212% | 6.743% | 90.262% | 10.109 | 7.391 |
| 19 | 700 | 650 | 0.005 | 700 | 325 | 0.886 | 65749 | 13.15% | 13333 | 2.67% | 512 | 0.10% | 16895 | 3.38% | 391933 | 78.39% | 11578 | 2.32% | 3.188% | 6.773% | 90.255% | 10.112 | 7.375 |
| 20 | 500 | 500 | 0.005 | 500 | 250 | 0.866 | 65597 | 13.12% | 24369 | 4.87% | 722 | 0.14% | 16449 | 3.29% | 391887 | 78.38% | 976 | 0.20% | 5.776% | 4.257% | 90.213% | 7.188 | 6.463 |
| | | | | | | | | | | | | | | | | | | | | | | | |
| 3821 | 600 | 450 | 0.005 | 50 | 563 | 0.346 | 65447 | 13.09% | 35 | 0.01% | 409130 | 81.83% | 1016 | 0.20% | 24347 | 4.87% | 25 | 0.01% | 94.158% | 4.100% | 5.603% | 53.826 | 4427 |
| 3822 | 600 | 450 | 0.01 | 50 | 563 | 0.346 | 65927 | 13.19% | 23 | 0.00% | 408554 | 81.71% | 1053 | 0.21% | 22152 | 4.43% | 2291 | 0.46% | 94.126% | 13.116% | 5.103% | 128.611 | 23924 |
| 3823 | 1000 | 850 | 0.005 | 100 | 975 | 0.222 | 65157 | 13.03% | 11 | 0.00% | 411962 | 82.39% | 897 | 0.18% | 21344 | 4.27% | 629 | 0.13% | 94.741% | 6.672% | 4.908% | 92.488 | 5811 |
| 3824 | 800 | 500 | 0.005 | 50 | 718 | 0.440 | 65429 | 13.09% | 22 | 0.00% | 412160 | 82.43% | 911 | 0.18% | 21118 | 4.22% | 360 | 0.07% | 94.848% | 5.677% | 4.860% | 43.496 | 2531 |
| 3825 | 900 | 800 | 0.01 | 100 | 873 | 0.243 | 65717 | 13.14% | 11 | 0.00% | 406282 | 81.26% | 1085 | 0.22% | 20798 | 4.16% | 6107 | 1.22% | 93.555% | 25.695% | 4.789% | 383.653 | 150438 |
| 3826 | 1000 | 1050 | 0.01 | 150 | 997 | 0.082 | 66030 | 13.21% | 8 | 0.00% | 406182 | 81.24% | 1177 | 0.24% | 20351 | 4.07% | 6252 | 1.25% | 93.599% | 26.742% | 4.689% | 199.142 | 7646 |
| 3827 | 900 | 500 | 0.01 | 50 | 761 | 0.535 | 65500 | 13.10% | 23 | 0.00% | 407282 | 81.46% | 1145 | 0.23% | 17951 | 3.59% | 8099 | 1.62% | 93.741% | 33.992% | 4.131% | 58.225 | 2676 |
| 3828 | 1000 | 500 | 0.01 | 50 | 801 | 0.599 | 65804 | 13.16% | 12 | 0.00% | 403926 | 80.79% | 1218 | 0.24% | 17887 | 3.58% | 11153 | 2.23% | 93.031% | 40.885% | 4.120% | 28.040 | 65 |
| 3829 | 800 | 500 | 0.01 | 50 | 718 | 0.440 | 65880 | 13.18% | 27 | 0.01% | 411665 | 82.33% | 937 | 0.19% | 16543 | 3.31% | 4948 | 0.99% | 94.834% | 26.240% | 3.811% | 75.963 | 5461 |
| 3830 | 1000 | 550 | 0.005 | 50 | 881 | 0.474 | 66168 | 13.23% | 12 | 0.00% | 415741 | 83.15% | 730 | 0.15% | 16257 | 3.25% | 1092 | 0.22% | 95.833% | 10.078% | 3.747% | 53.311 | 5468 |
| 3831 | 1000 | 850 | 0.01 | 100 | 975 | 0.222 | 65330 | 13.07% | 12 | 0.002% | 412098 | 82.42% | 871 | 0.17% | 15910 | 3.18% | 5779 | 1.16% | 94.810% | 29.477% | 3.660% | 256.684 | 37704 |
| 3832 | 700 | 500 | 0.005 | 50 | 674 | 0.272 | 65630 | 13.13% | 19 | 0.004% | 419413 | 83.88% | 589 | 0.12% | 14309 | 2.86% | 40 | 0.01% | 96.561% | 4.211% | 3.294% | 71.500 | 12637 |
| 3833 | 900 | 550 | 0.005 | 50 | 837 | 0.368 | 65986 | 13.20% | 18 | 0.004% | 420144 | 84.03% | 543 | 0.11% | 12947 | 2.59% | 362 | 0.07% | 96.808% | 6.533% | 2.983% | 55.009 | 2629 |
| 3834 | 700 | 500 | 0.01 | 50 | 674 | 0.272 | 65828 | 13.17% | 14 | 0.003% | 418994 | 83.80% | 585 | 0.12% | 12729 | 2.55% | 1850 | 0.37% | 96.507% | 16.058% | 2.932% | 100.957 | 3266 |
| 3835 | 1000 | 550 | 0.01 | 50 | 881 | 0.474 | 65808 | 13.16% | 16 | 0.003% | 416421 | 83.28% | 687 | 0.14% | 11242 | 2.25% | 5826 | 1.17% | 95.911% | 36.683% | 2.589% | 91.629 | 6668 |
| 3836 | 900 | 550 | 0.01 | 50 | 837 | 0.368 | 65775 | 13.16% | 16 | 0.003% | 420351 | 84.07% | 558 | 0.11% | 9775 | 1.96% | 3525 | 0.71% | 96.809% | 29.463% | 2.251% | 135.650 | 13985 |
| 3837 | 1000 | 600 | 0.005 | 50 | 961 | 0.277 | 65848 | 13.17% | 8 | 0.002% | 427627 | 85.53% | 269 | 0.05% | 6052 | 1.21% | 196 | 0.04% | 98.499% | 7.135% | 1.394% | 101.737 | 18564 |
| 3838 | 800 | 550 | 0.005 | 50 | 790 | 0.156 | 65524 | 13.10% | 11 | 0.002% | 428332 | 85.67% | 236 | 0.05% | 5867 | 1.17% | 30 | 0.01% | 98.588% | 4.337% | 1.350% | 87.917 | 8513 |
| 3839 | 800 | 550 | 0.01 | 50 | 790 | 0.156 | 65207 | 13.04% | 7 | 0.001% | 428814 | 85.76% | 251 | 0.05% | 4882 | 0.98% | 839 | 0.17% | 98.626% | 18.252% | 1.123% | 195.014 | 16000 |
| 3840 | 1000 | 600 | 0.01 | 50 | 961 | 0.277 | 65586 | 13.12% | 11 | 0.002% | 427651 | 85.53% | 296 | 0.06% | 4658 | 0.93% | 1798 | 0.36% | 98.446% | 31.013% | 1.072% | 226.342 | 40309 |

Table 4: Dependence of $\boldsymbol{\eta}$ from $L$ and $\boldsymbol{\sigma_{err}}$.

| $L$ [mm] | $\eta$ [%] | | |
|---|---|---|---|
| | $\sigma_{err}$ =0.005mm | $\sigma_{err}$ =0.01mm | Gap |
| 50 | 21.468% | 17.227% | 4.241% |
| 100 | 35.103% | 28.149% | 6.954% |
| 150 | 44.465% | 35.948% | 8.517% |
| 200 | 50.718% | 40.766% | 9.952% |
| 250 | 55.610% | 44.188% | 11.423% |
| 300 | 60.049% | 47.626% | 12.423% |
| 350 | 61.918% | 48.110% | 13.808% |
| 400 | 65.090% | 50.614% | 14.476% |
| 450 | 66.357% | 50.201% | 16.156% |
| 500 | 68.722% | 51.918% | 16.804% |
| 550 | 69.477% | 51.042% | 18.435% |
| 600 | 71.596% | 52.595% | 19.002% |
| 650 | 71.427% | 50.988% | 20.440% |
| 700 | 72.510% | 51.780% | 20.730% |
| 750 | 72.834% | 50.592% | 22.241% |
| 800 | 73.403% | 50.979% | 22.425% |
| 850 | 72.976% | 49.454% | 23.521% |
| 900 | 73.467% | 49.773% | 23.694% |
| 950 | 72.867% | 48.299% | 24.569% |
| 1000 | 72.506% | 48.039% | 24.466% |

performances, i.e. $\eta < 30\%$. Optimal conditions are, respectively, for reflector length of 800 mm and $\sigma_{err} = 0.005$ mm and of 600 mm for $\sigma_{err} = 0.01$ mm. A significant performance increase occurs for values of $L$ included in $[50{,}450]$ mm range, while for higher values of the reflector length, i.e. $L > 500$ mm, the global transfer efficiency presents comparable values.

Finally, considering the gap between the performances in the trends identified by the two values of $\sigma_{err}$, an increase, from 4.241% to 24.466%, occurs. High values of $\sigma_{err}$ have a crucial impact on the global transfer efficiency in presence of high values of $L$. Long reflectors force the emitted rays to cover long trajectories from the source to the mirror and, then, from the mirror to the target. An error, caused by anomalies in the mirror surface, generates an angular deviation of the ray path. This deviation is amplified by the distance between the mirror and the target. Consequently, if $L$ increases the standard deviation of the dispersion azimuthal angular error distribution must have low values not to significantly reduce the values of $\eta$.

Another relevant parameter for the effective mirror reflector design is the ellipsoid eccentricity, $\varepsilon$, defined in previous Eq. (9) and included in the $[0{,}1]$ range. It identifies the mutual position of the vertices and the foci. If $\varepsilon$ is equal to 0 the ellipsoid is a sphere, i.e. $A = B$, values of $\varepsilon$ between 0 and 1 are for eccentric geometries where $B < A$. If $\varepsilon = 1$ the ellipsoid degenerates into a plane and the foci lay upon the vertices on the major axis.

Developed *what-if analysis* highlights a range of optimal values for the ellipsoid eccentricity, to maximize the global transfer efficiency, included between 0.75 and 0.9, as represented in Figure 8, correlating the ellipsoidal mirror eccentricity to the values of $\eta$. Each dot represents one of the 3840 simulated scenario.

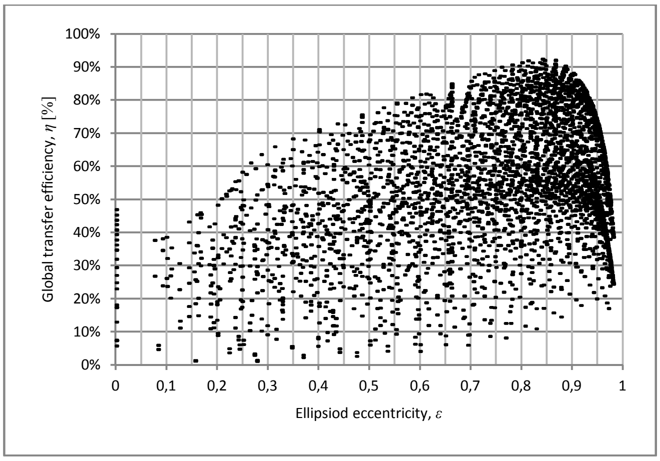


Figure 8: Correlation between the Ellipsoid Eccentricity and Global Transfer Efficiency.

This outcome may be in contrast to the major literature (Steinfeld and Fletcher (1988), Steinfeld (1991)) suggesting low values of $\varepsilon$ to maximize the reflector global transfer efficiency. On the contrary, in the proposed analysis values of eccentricity close to zero generate the worst performances. A reasonable explanation for this evidence lies in the adopted reflector modeling approach. Literature ray-tracing models and related results approximate the reflector with an ellipsoid of revolution neglecting both the truncation section, i.e. the parameter previously called $TD$, and the hole necessary to install the light source. The proposed ray-tracing approach includes these two elements in the analytical model to provide a realistic and accurate description of the physical system.

The presence of these elements significantly modifies the geometric and optic features of the solar simulator introducing the so-called losses at the reflector stage (see Figure 3) that significantly contribute to the global transfer efficiency decrease, especially for the scenarios where $L$ and $\varepsilon$ assume low values (see Table 3). In fact, if $\varepsilon$ is low the foci are located far from the vertices on the ellipsoid major axis and close to the geometrical center, i.e. the point of intersection of the two axes. In this circumstance, the light source, located on one ellipsoid focus point, juts out from the reflector profile so that a large number of the emitted rays do not hit the reflector surface. The lower the reflector length, the higher these losses occur.

On the contrary, in eccentric reflectors the light source is close to the ellipsoid major axis vertex and a lower number of rays are lost. However, very high values of $\varepsilon$, i.e. $\varepsilon > 0.9$, cause an increase of the losses at the reflector stage and a decrease of $\eta$. This is due to the presence of the hole for the light source installation. A focus point located close to the reflector vertex, i.e. eccentric reflector, increases the value of $N_H$, i.e. the number of rays lost due to the presence of the hole used to install the light source, so that, also in this case, the global transfer efficiency decreases. As introduced, optimal values for the reflector eccentricity are in the $[0.75,0.9]$ range.

## 5. CONCLUSIONS AND FURTHER RESEARCH

This paper presents a Monte Carlo ray-tracing approach facing the effective design of solar simulators. Developed model reproduces the trajectories of light rays considering the main physical and optic phenomena that occur from the source to the target area. Ellipsoidal geometries are focused. In particular, the solar simulator reflector is a truncated ellipsoid of revolution with the light source located on one focus and the target area on the other. Proposed ray-tracing approach includes the main losses at the source, reflector and target stages and affecting the global system transfer efficiency.

The ray-tracing approach is integrated to a Monte Carlo *what-if* analysis to simulate the performances of several reflector geometries. A case study, based on an OSRAM XBO® 3000W/HTC OFR Xenon short arc lamp, is described simulating 3840 scenarios and varying four major parameters, i.e. the ellipsoid major axis, the truncation diameter, the reflector length and the standard deviation of the azimuthal angular error distribution affecting the quality and reflectivity of the mirror surface. For each scenario, data about losses and the number of rays on target are collected and summarized in the three key indices proposed in Eq. (6) to (9) together with a statistic analysis of the distribution of rays on target.

The main outcomes highlight the relevance of the proper design of the reflector shape to obtain high values of the global transfer efficiency. The gap between the best and worst scenarios is higher than 90%. Furthermore, correlations between the four considered parameters is highlighted. As example, high values of the reflector length, in presence of high values of the standard deviation of the azimuthal angular error distribution, amplify the global transfer efficiency decrease, while, low values of the ellipsoid eccentricity, relating the major axis length to the truncation diameter, cause an increase of the lost rays.

The obtained parameters, for the best of the simulated scenarios, are of 600 mm for both the ellipsoid major semi-axis and reflector length, 325 mm for minor semi-axis and $\sigma_{err}$ equals to 0.005 mm. For this scenario, the global transfer efficiency is 92.407% while the distribution of rays on the target area has a mean distance from the focus point of 8.284 mm and a standard error of 6.387 mm.

Further research mainly deals with a validation of the case study results through the development of the solar simulator and a trial campaign. To this purpose, the authors already purchased the ellipsoidal reflector and they are now developing the overall structure of the solar simulator to collect experimental data to be compared to the Monte Carlo simulation evidences.

## REFERENCES


Amoh, H., 2004. Design for multi-solar simulator. *Proceedings of SPIE – The International Society for Optical Engineering*. 5520. pp. 192-199. August 4-6, Denver (Colorado, USA).

Chen, C.F., Lin, C.H., Jan, H.T., 2010. A solar concentrator with two reflection mirrors designed by using a ray tracing method. *Optik*, 121, 1042–1051.

Codd, D.S., Carlson, A., Rees, J., Slocum, A.H., 2010. A low cost high flux solar simulator. *Solar Energy*, 84, 2202–2212.

Cooper, T., Steinfeld, A., 2011. Derivation of the angular dispersion error distribution of mirror surfaces for Monte Carlo ray-tracing applications. *Journal of Solar Energy Engineering*, 133 (4), 44501 1-4.

Domínguez, C., Antón, I., Sala, G., 2008. Solar simulator for concentrator photovoltaic systems. *Optics express*, 16 (19), 14894–14901.

Domínguez, C., Askins, S., Antón, I., Sala, G., 2009. Characterization of five CPV module technologies with the Helios 3198 solar simulator. *IEEE*, 1004–1008.

Hussain, F., Othman, M.Y.H., Yatim, B., Ruslan, H., Sopian, K., 2011. Fabrication and irradiance mapping of low cost solar simulator for indoor testing of solar collector. *Journal of Solar Energy Engineering*, 133 (4), 44502 1–4.

Johnston, G., 1995. On the analysis of surface error distributions on concentrated solar collectors. *Transations of the ASME*, 117, 294–296.

Kruger, K.R., Davidson, J.H., Lipiński, W., 2011. Design of a new 45 kWe high-flux solar simulator for high-temperature solar thermal and thermo-chemical research. *Journal of Solar Energy Engineering*, 133 (4), 11013 1–8.

Meng, Q., Wang, Y., Zhang, L., 2011a. Irradiance characteristics and optimization design of a large-scale solar simulator. *Solar Energy*, 85, 1758–1767.

Meng, Q., Wang, Y., 2011b. Testing and design of a low-cost large scale solar simulator. *Proceedings of SPIE – The International Society for Optical Engineering*, 8128, August 22-23, San Diego (California, USA).

Osram, *Technical information No. 5264*. Available from: http://www.osram.com [accessed May 2012].

Ota, Y., Nishioka, K., 2010. 3-dimensional simulator for concentrator photovoltaic modules using ray-trace and circuit simulator. *Proceedings of the 35th IEEE Photovoltaic Specialists Conference,* *PVSC 2010*, pp. 3065-3068, June 20-25, Honolulu (Hawaii, USA)

Petrash, J., Coray, P., Meier, M., Brack, M., Häberling, P., Wuillemin, D., Steinfeld, A., 2007. A novel 50 kW 11.000 suns high-flux solar simulator based on an array of xenon arc lamps. *Journal of Solar Energy Engineering*, 129, 405–411.

Pravettoni, M., Galleano, R., Dunlop, E.D., Kenny, R.P., 2010. Characterization of a pulsed solar simulator for concentrator photovoltaic cell calibration. *Measurement Science and Technology*, 21, 1–8.

Renh, H., Hartwig, U., 2010. A solar simulator design for concentrating photovoltaics. *Proceedings of SPIE – The International Society for Optical Engineering*, 7785, August 1-4, San Diego (California, USA).

Steinfeld, A., 1991. Exchange factor between two spheres placed at the foci of a specularly reflecting ellipsoidal cavity. *International Communications in Heat and Mass Transfer*, 18, 19–26.

Steinfeld, A., Fletcher, E.A., 1988. Solar energy absorption efficiency of an ellipsoidal receiver-reactor with specularly reflecting walls. *Energy*, 13 (8), 609–614.